Self-assembly of functionally gradient nanoparticle structures

Jonghyun Park and Wei Lu[a)]
Department of Mechanical Engineering, University of Michigan, Ann Arbor, Michigan 48109, USA

(Received 3 October 2008; accepted 19 November 2008; published online 15 December 2008)

Morphology control of binary nanoparticles in an electric field was investigated by a computational model. The study revealed rich patterning dynamics and how collective actions of relative permittivity, volume fraction, and particle size can lead to a wide range of superlattice structures from functionally gradient columns to chain networks. These results suggest a significant degree of experimental control to assemble binary nanoparticles into new materials. © *2008 American Institute of Physics*. [DOI: 10.1063/1.3049351]

Self-assembly of nanoparticles into superlattice structures is a promising approach to construct functional materials or novel devices.[1–3] Among a variety of driving forces for self-assembly, electrostatic interaction plays an important role due to its long-range nature and easiness of control.[4,5] Electric field can cause organized nanostructures in an electroreological fluid,[6] which is composed of nanoparticles dispersed in a nonconducting liquid. The monodispersed spherical particles tend to line up and form a chain parallel to the applied field.[6] Such a behavior can be attributed to the electric polarization interaction, a pairwise dipolar interaction, between particles. The potential energy of the system depends on the orientation of the superlattice with respect to the applied field, the arrangement of the particles, and the distance between the particles. Tao and Sun[7] suggested that under a strong field, the ground state of the superlattice has a body-centered-tetragonal (BCT) structure, which has been observed in simulations[8] and experiments.[9] The phase diagram for dipolar hard spheres obtained from Monte Carlo simulations shows the possibility of multiple phases including fluidic, face-centered-cubic, hexagonal-close-packed, and BCT phases.[10]

The superlattice structures of binary nanoparticles can lead to a wide class of nanocomposite materials with properties not attainable by a single particle component. The behavior of binary nanoparticles in an electric field is still not well understood. The goal of this paper is to elucidate how parameters such as relative permittivity, volume fraction, and particle size can be utilized to tune the superlattice structures.

We employ Brownian dynamics[11] to model the formation of nanoparticle superlattice structures. The trajectories of the particles are governed by the Langevian equation, $m_i\ddot{\mathbf{r}}_i(t)=\mathbf{F}_i^D+\mathbf{F}_i^R+\mathbf{F}_i^E$. Here m_i and $\mathbf{r}_i$ denote the mass and position of particle i. The left side of this equation, i.e., the inertia term, can be neglected for nanoparticles due to the small size and corresponding low Reynolds number. The vector $\mathbf{F}_i$ is the force acting on the particle, with superscripts D, R, and E denoting the drag force, random force, and electrostatic force, respectively. The Stoke's law gives $\mathbf{F}_i^D=-3\pi\eta d_i\mathbf{v}_i$, where η is the viscosity of the medium, while d_i and $\mathbf{v}_i$ denote the diameter and velocity of particle i. The random force $\mathbf{F}_i^R(t)$ has a Gaussian distribution and obeys the fluctuation dissipation theorem, giving $\langle\mathbf{F}_i^R(t)\cdot\mathbf{F}_i^R(t')\rangle=6\pi\eta d_i k_B T\delta(t-t')$,[11] where t and t' are time, k_B is Boltzmann's constant, and T is the absolute temperature. Each particle will acquire an effective induced dipole in an applied electric field $\mathbf{E}$, given by

$$\mathbf{p}_i=\frac{\pi d_i^3}{2}\frac{\varepsilon_i-\varepsilon_m}{\varepsilon_i+2\varepsilon_m}\varepsilon_m\mathbf{E}, \tag{1}$$

where ε_i and ε_m are the dielectric permittivities of particle i and the medium, respectively. The interactive energy between two dipoles, $\mathbf{p}_i$ and $\mathbf{p}_j$, is given by

$$U(\mathbf{r}_{ij})=\frac{1}{4\pi\varepsilon_m|\mathbf{r}_i-\mathbf{r}_j|^3}[\mathbf{p}_i\cdot\mathbf{p}_j-3(\mathbf{n}\cdot\mathbf{p}_i)(\mathbf{n}\cdot\mathbf{p}_j)], \tag{2}$$

where $\mathbf{r}_i$ is the position vector of particle i and $\mathbf{n}$ is a unit vector in the direction of $\mathbf{r}_j-\mathbf{r}_i$.

Consider the assembly of nanoparticles confined in between two parallel electrodes, separated by a distance L with an applied voltage V. Attach a coordinate to the grounded electrode, with the x,y axes in the plane while the perpendicular z axis pointing to the other electrode. This configuration leads to a uniform applied electric field $E=V/d$, which can be used in Eq. (1). Note that the dipoles in the particles can disturb this uniform field when they are close to an electrode and cause electrons in the electrode to redistribute. As a result, the electric field becomes nonuniform. To consider this effect, we employ the image charge method.[12] Image charges are placed systematically so that the isopotential condition on the electrodes can be satisfied. For any particle carrying dipole $\mathbf{p}_i$ at position $\mathbf{r}_i=(x_i,y_i,z_i)$, we put a series of image dipoles of the same $\mathbf{p}_i$ at positions $(x_i,y_i,-z_i)$ and $(x_i,y_i,2kL\pm z_i)$, where $k=\pm1,\pm2,\ldots$ is a nonzero integer. In addition to the dipole interaction between particles, these image dipoles also interact with the particles. Thus the near-electrode effect is included by considering the interaction among all dipoles. The electrostatic forces are given by $\mathbf{F}_i^E=-\nabla\Sigma_{j,j\neq i}U(\mathbf{r}_{ij})$, where j summates over all dipoles.

In the simulation a cutoff length has been used when calculating the electrostatic force on a particle. A sphere centered at the particle with the cutoff length as the radius defines a domain. Only dipoles inside this domain are counted toward the contribution. This cutoff length also determines the necessary range of k for the image dipoles since only k with corresponding image dipoles in the domain are relevant. We introduced a short-range repulsive potential to ensure no penetration between particles as well as electrodes.

a)Author to whom correspondence should be addressed. Electronic mail: weilu@umich.edu.

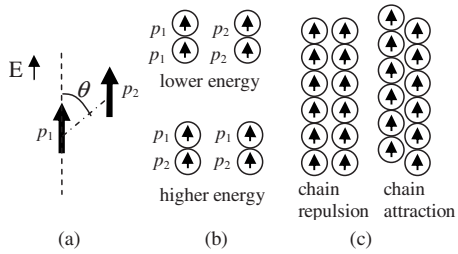

FIG. 1. (a) Interaction between two dipoles. (b) Forming chains of same kind particles is energetically favorable. (c) Interaction between chains depends on the relative position.

Use subscript "1" to denote a reference particle. Its diameter d_1 defines a length scale. The competition between the electrostatic force and the drag force defines a time scale,

$$\tau = \frac{\eta}{\varepsilon_m (\alpha E)^2}. \tag{3}$$

Here αE can be treated as an effective electric field, where $\alpha = (\varepsilon_1 - \varepsilon_m)/(\varepsilon_1 + 2\varepsilon_m)$ is a dimensionless parameter that reflects the effect of dielectric permittivity. The electrostatic force versus the random force defines a dimensionless number,

$$\Lambda = d_1^{3/2} \alpha E \sqrt{\frac{\varepsilon_m}{k_B T}}. \tag{4}$$

Thus larger electric field or particle diameter reduces the relative contribution from the Brownian motion. Brownian motion can shake the nanoparticles to avoid them being trapped in a local energy minimum. Thus an appropriate Λ could be helpful to form more ordered structures. On the other hand, a system may lose its order when Λ is too small due to the random movement of particles.

Insight into the particle assembly behavior can be obtained by looking into the particle interaction. Define the permittivity ratios of the particles and the medium by $\beta_1 = \varepsilon_1/\varepsilon_m$ and $\beta_2 = \varepsilon_2/\varepsilon_m$. Equation (1) suggests that the effective dipole follows the applied electric field direction when a particle is more polarizable than the medium, or $\beta_1 > 0$. The effective dipole points to the opposite direction of the electric field when $\beta_1 < 0$. The second term in the bracket of Eq. (2) shows orientation dependence. In terms of the angle θ shown in Fig. 1(a), the interactive energy scales as $-p_1 p_2 \cos^2 \theta$. For two particles of the same kind, the energy will always be minimized when the two particles line up along the electric field direction so that $\theta = 0$ or π, no matter whether they are more polarizable than the medium or not. It becomes intriguing when considering the interaction of two particles of different kinds, which can be summarized into two cases: (1) both particles are more polarizable $(\beta_1, \beta_2 > 1)$ or less polarizable $(\beta_1, \beta_2 < 1)$ than the medium and (2) one particle is more polarizable than the medium $(\beta_1 > 1)$ while the other is less polarizable $(\beta_2 < 1)$.

In the first case, the interactive energy is lower when two particles line up along the electric field, similar to the situation for the same kind of particles. As a result, nanoparticles tend to form a chain along the field direction. Eventually the chain can bridge the electrodes if there are enough particles. Beyond that multiple chains can form. When particles have a similar size, it can also be shown that the formation of pure chains each composed of a single kind of particles is energetically favorable. Consider the two arrangements shown in Fig. 1(b). The energy for the configuration above scales as $-(p_1^2 + p_2^2)$, which is always lower than the energy for the configuration below, which scales as $-2p_1 p_2$. When two chains are close, the interaction depends on their relative position. Figure 1(c) shows that there is chain-chain repulsion for the configuration on the left. However, two chains would attract each other in a configuration shown on the right. This transition can be understood by calculating the interaction between an infinitely long chain and a particle. Consider a straight line linking the centers of this particle and its nearest neighbor on the chain. Define the angle between this line and the chain direction by ϕ. To simplify the discussion assume the particles have the same size so that we only need to consider $60° \leqslant \phi \leqslant 90°$ due to symmetry. Our calculations show that the chain attracts the particle when $60° \leqslant \phi \leqslant 75.6°$ and repels the particle when $75.6° \leqslant \phi \leqslant 90°$. The attraction can drive individual chains to assemble into columns.

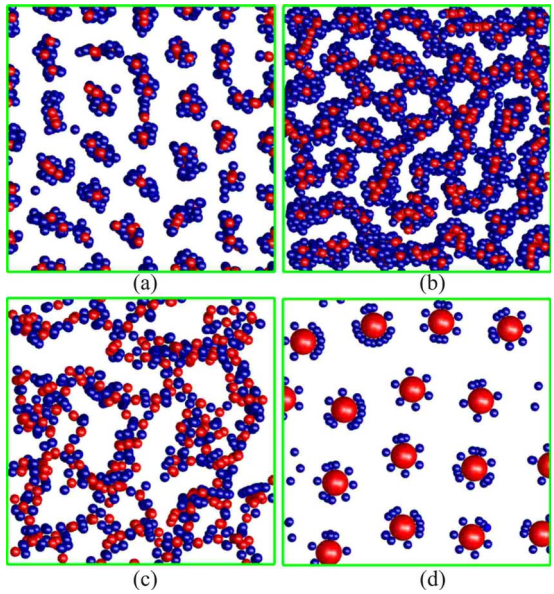

FIG. 2. (Color online) Top view of structures by red (subscript 1) and blue (subscript 2) particles. (a) $\beta_1 = 50$, $\beta_2 = 5$, $\Lambda = 175$, and $N = 2000$. (b) $\beta_1 = 50$, $\beta_2 = 5$, $\Lambda = 175$, and $N = 6000$. (c) $\beta_1 = 2.8$, $\beta_2 = 0.28$, $\Lambda = 175$, and $N = 2000$. (d) Single layer $\beta_1 = 50$, $\beta_2 = 5$, $\Lambda = 50$, and $N = 200$.

In the second case, however, the opposite direction of the polarization leads to an interactive energy scales as $p_1 p_2 \cos^2 \theta$. Thus the energy is lower when $\theta = 90°$. Two particles would prefer to stay in a plane perpendicular to the field direction and attract each other. The discussion in Fig. 1(c) would be reversed: the chain-chain interaction would be attractive for the configuration on the left and repulsive for the configuration on the right.

Representative results are shown in Fig. 2. Periodic boundary conditions were used in the x and y directions. The systems were allowed to evolve for a long time until no significant changes could be observed. Figure 2(a) shows a top view of the structure in the (x, y) plane. Behind each visible particle shown in the figure is a particle chain lining up in the z direction. The two kinds of particles are denoted by red (subscript 1) and blue (subscript 2) colors. They have the same diameter and are both more polarizable than the medium with $\beta_1 = 50$ and $\beta_2 = 5$. The system has $N = 2000$ particles. The spacing between the electrodes is $L = 14 d_1$ and

the calculation cell size is $27d_1 \times 27d_1 \times 14d_1$. Thus the volume fraction of particles is 10.2%. Under these situations the particles assemble into isolated columns with a core-shell configuration. The core is composed of the more polarizable red particles, while the shell is composed of the blue ones. From an energetic point of view, the attraction between two red particle chains is stronger than the interaction between a red particle chain and a blue particle chain. The latter is stronger than the attraction between two blue particle chains. As a result, the red chains aggregate to form columns. The blue chains tend to get close to the red columns as much as possible, leading to the formation of shells. It is exciting to note that this self-organized functionally gradient structure offers a gradual transition of the permittivity from that of the core to that of the medium. This approach could be potentially very useful to construct functional gradient nanocomposites from the bottom up.

Figure 2(b) shows the simulation for a higher volume fraction of particles. The number of particles is 6000, leading to a volume fraction of 30.6%. The system evolves into a continuous structure with isolated holes in between. The blue particles enclose the red particles and form the peripheral regions around the holes. We observed from simulations that in both Figs. 2(a) and 2(b), the particle columns demonstrate local BCT structures. Another common feature is that the same kind of particles tends to aggregate.

Figure 2(c) demonstrates the structure when one kind of particle is more polarizable than the medium while the other is less polarizable. The parameters are the same as those in Fig. 2(a), except that the red particle has $\beta_1 = 2.8$ while the blue particle has $\beta_2 = 0.28$. The particles also form pure chains along the field direction with each chain composed of single kind particles. A distinct feature in Fig. 2(c) is that the red and blue chains are highly dispersed and form a network. This morphology is in contrast to that in Fig. 2(a), where the same color chains aggregate. As mentioned before, the opposite dipole directions cause the red and blue particles to stay in a plane perpendicular to the field direction, which minimizes the interactive energy with $\theta = 0$. In the plane of the same kind of particles, they repel each other, while different kinds of particles attract each other. As a result, particles appear more dispersed.

Assembling a single layer of nanoparticles on a substrate has many potential applications. A relevant simulation is shown in Fig. 2(d) for a layer of two kinds of particles. The parameters are the same as those in Fig. 2(a) except that the diameter of the red particle is three times as large, and the system is much dilute with 16 red particles among 200. Equations (1) and (2) suggest that the interaction increases quickly with the particle diameter. Thus stronger interaction between red particles is expected. Initially we put the red and blue particles randomly on one electrode surface. We find that the interaction between the red particles and electrode can hold them on the surface. As time goes by, the repulsion between the red particles leads them to form a nicely ordered triangular lattice. The attraction between the blue and red particles causes the formation of blue rings surrounding the red cores.

In summary, our model shows several essential features of the structures formed by binary nanoparticle systems under an electric field. Assembling different nanoparticles systematically into ordered binary superlattices can lead to more complex materials from which multifunctionalities may emerge. The predicted structures may provide some critical insight into materials design indispensible for making such engineered structures feasible.

The authors acknowledge financial support from National Science Foundation CAREER Award No. DMI-0348375.

[1] A. P. Alivisatos, Science **271**, 933 (1996).
[2] S. A. Maier, Nature Mater. **2**, 229 (2003).
[3] J. Hoinville, J. Appl. Phys. **93**, 7187 (2003).
[4] W. Lu and D. Salac, Phys. Rev. Lett. **94**, 146103 (2005).
[5] J. Park and W. Lu, Appl. Phys. Lett. **91**, 053113 (2007).
[6] M. Parthasarathy and D. J. Klingenberg, Mater. Sci. Eng., R **17**, 57 (1996).
[7] R. Tao and J. M. Sun, Phys. Rev. Lett. **67**, 398 (1991).
[8] R. Tao and Q. Jiang, Phys. Rev. Lett. **73**, 205 (1994).
[9] T. Chen, R. N. Zitter, and R. Tao, Phys. Rev. Lett. **68**, 2555 (1992).
[10] A. Hynninen and M. Dijkstra, Phys. Rev. E **72**, 051402 (2005).
[11] M. P. Allen and D. J. Tildesley, *Computer Simulation of Liquids* (Clarendon, Oxford, 1987).
[12] M. N. O. Sadiku, *Elements of Electromagnetics* (Oxford University Press, Oxford, 2006).